SHEAR PERFORMANCE OF SPECIAL DRY JOINTS FOR PRECAST CONCRETE SEGMENTS

Watanachai Smittakorn[1], Tosporn Prasertsri[1*], Worapon Pattharakorn[1], and Pitcha Jongvivatsakul[2]

[1]Applied Mechanics and Structures Research Unit, Department of Civil Engineering, Faculty of Engineering, Chulalongkorn University, Bangkok, Thailand,
e-mail: watanachai.s@chula.ac.th, tosporn.p@chula.ac.th, worapon.wp23@gmail.com

[2]Innovative Construction Materials Research Unit, Department of Civil Engineering, Faculty of Engineering, Chulalongkorn University, Bangkok, Thailand,
e-mail: pitcha.j@chula.ac.th

Received Date: June 25, 2020; Revised Date: August 7, 2020; Acceptance Date: October 5, 2020

Abstract

The special dry joints for precast prestressed concrete segments are invented in this study to overcome the limitation of conventional dry joints. Eight specimens of special dry joints were made and subjected to direct shear test. Test parameters comprise concrete compressive strength (normal and high strength concrete) and steel fiber volume added in the special dry joint (0%, 0.5%, and 1.0%). Test results revealed that the inclusion of steel fibers remarkably enhanced the shear capacity and ductility index. Failure mode of specimens was changed from shearing off to concrete cracking around shear key corners, defined as ductile shearing-off failure. Furthermore, the existing equations for predicting shear capacity of keyed joints were validated by the experimental results. Among available equations from literatures, the Turmo's equation yields better prediction of the shear capacity for the special dry joint made with normal strength concrete.

Keywords: Dry joint, Precast prestressed concrete, Shear behavior, Shear key, Steel fibers

Introduction

Precast segmental box girders are widely used in modern bridge construction due to its advantages over the cast-in-place construction such as cost-saving from extensive formworks, reducing on-site environmental impact, and eliminating the time during the concrete casting process. Connections, the crucial parts in precast system, can be constructed using various techniques, such as monolithic placement [1-3], epoxy-bonding connection [4-8], and dry joint [4, 9-12]. Based on experimental results from previous studies, the monolithic placement and epoxy-bonding connection offer high shear capacity [1-3]. However, they consume time for the hardening process of cementitious or adhesive substances, whereas epoxy-bonding connection exhibits brittle failure behavior [13].

Dry joints, where the precast segments are connected without any binder, can help reducing the construction time. Even though the shear capacity is lower than that of epoxy-bonding connection, its failure mechanism is less brittle [7]. Shear keys are normally used in dry joints to achieve satisfactory connectivity performance. Investigations in the past proved that shear key systems are able to reduce the swelling of wood-concrete composite beams and also resist permanent deformation under cyclic loading without strength degradation [14-16]. The biggest problem of dry joints with shear keys is the imperfect fit of shear keys since segments are cast separately [17]. Attempts have been made to alleviate such a problem by applying the match-cast method to the precast segments. However, the dry joints are still found not well-fitted together. In order

to overcome this problem, a special dry joint for precast concrete connection is presented in this study. In addition, the previous works suggested that concrete compressive strength and fiber proportion affected the shear capacity of concrete joints [5, 7, 13, 18-24].

The objective of this study is to investigate the shear capacity of the proposed special dry joints made with various concrete mixtures. The effects of concrete compressive strength and steel fiber volume are examined through direct shear tests. Shear performance is assessed from load carrying capacity and ductility index at maximum load of specimens. Furthermore, the applicability of shear capacity equations from literatures is verified with the experimental results in this study.

Experimental Program

Specimens

The details of specimen and reinforcement are given in Figure 1. The thickness of specimens was 200 mm. The special dry joints consisted of three shear keys and steel reinforcement, as shown in Figure 1(a). The joints were cast in advance by match-cast, and then they were fabricated into specimens, as shown in Figure 1(b). Reinforcing ribbed and dowel bars were the deformed bar with diameter 12 mm (DB12). Round bars with diameter 9 mm (RB9) were used to confine the reinforcing bar in the specimens.

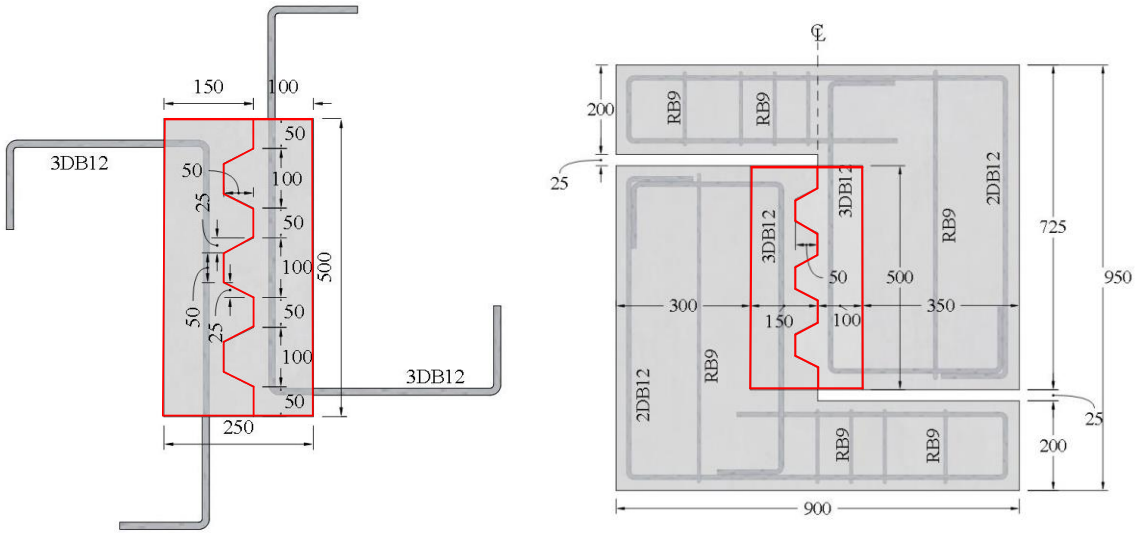

(a) Special dry joint (b) Test specimen

Figure 1. Specimen geometry and reinforcing steel detailing (dimensions in mm.)

Figure 2 presents the casting procedures of special dry joints. First, the steel mold with three shear keys was prepared as shown in Figure 2(a). Next, a concrete mixture was prepared and cast into steel formwork in Figure 2(a) to be female part of specimens. After concrete hardened, this female part was assembled with steel formwork and was used as mold for male part (see Figure 2(b)). Finally, male part was cast as illustrated in Figure 2(c). The surface of dry joint perfectly matches by using this method.

After preparing the special dry joint, the dry joint was installed to the formwork (Figure 3(a)) and the synthetic resin emulsion under the tradename LANKO 751 was applied at interface to improve bonding. The remaining concrete portion of specimens were cast as shown in Figure 3(b). The mix proportion of concrete for this part consists of 328 kg/m^3 of

Portland cement, 1,060 kg/m^3 of coarse aggregate, 890 kg/m^3 of fine aggregate, and 190 kg/m^3 of water. The target compressive strength of this concrete portion is 30 MPa. All specimens were cured with water and covered by wet cloth for 28 days.

(a) Steel formwork for casting

(b) Female part of specimen after casting

(c) Male part of specimen during casting

Figure 2. Casting of special dry joint

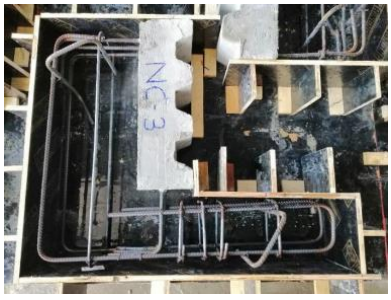

(a) Reinforcing steel placed

(b) Specimen after casting

Figure 3. Casting of test specimens

Materials

The concrete mixture proportions of the special dry joints are presented in Table 1. There are four experimental cases. The test variables included the concrete compressive strength and steel fiber volume. The control specimen was the mix NC which was normal strength concrete without steel fibers. Meanwhile, the steel fibers were added at 0.5% and 1% by concrete volume to the mix NC-0.5SF and NC-1SF, respectively. The target compressive strength of the mix NC, NC-0.5SF, and NC-1SF was 35 MPa, while the mix HC was targeted at 65 MPa. A polycarboxylate-based superplasticizer was used to maintain the concrete consistency of the mix HC.

Table 1. Mix Proportions of the Tested Specimens

Specimen	Portland Cement (kg/m^3)	Coarse Aggregate (kg/m^3)	Fine Aggregate (kg/m^3)	Water (kg/m^3)	Superplasticizer (ml)	Steel Fiber (kg/m^3)
NC	434	1,040	628	216	-	-
NC-0.5SF						39.3
NC-1SF						78.6
HC	594	1,090	540	180	156	-

The steel fibers under the trade name Dramix® RC 65/35 BN were used in this study. The diameter and length of steel fibers were 0.55 mm and 35 mm, respectively. The fibers had an aspect ratio of 65. Fiber shape was straight with hooked end. The tensile strength and elastic modulus of fibers were 1,100 MPa and 210,000 MPa, respectively.

The compressive strengths of the special dry joints are presented in Table 2. Each value is the average compressive strength of three cylindrical concrete specimens. The remaining concrete portions of specimens had a compressive strength of 32.1 MPa. Tensile properties of the reinforcing steel bars used in this study were tested according to ASTM A615 [25]. The average yield strength of the steel coupons obtained from RB9 and DB12 were 439 and 538 MPa, respectively. The RB9 and DB12 coupons had an average tensile strength of 483 and 777 MPa, respectively.

Table 2. Concrete Compressive Strength of the Special Dry Joints

Specimen	f_c' (MPa)
NC	48.6
NC-0.5SF	48.4
NC-1SF	46.5
HC	75.1

Test Setup and Instrumentation

The test configuration is depicted in Figure 4(a). A universal testing machine with a maximum load capacity of 5 MN was used for monitoring shear behavior of the specimens. Load was applied vertically on top surface of specimen to create shear force at connection. A load cell with a maximum capacity of 2 MN was installed on top of the specimens to measure the applied load. To simulate the transfer of prestressing force from tendon to concrete member, the confining stress of 1 MPa was applied constantly throughout.

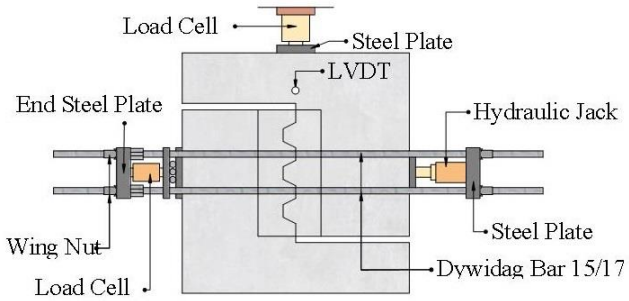

(a) Instrumentation

(b) Applied confining stress

(c) Loading condition

Figure 4. Test setup

The use of the confining stress of 1 MPa is consistent with the experiments conducted in the literatures [9, 26, 27]. Furthermore, the confining stress of 1 MPa is the upper bound value applied as transferred posttensioning stress in adjacent box girder bridges [28, 29]. The threaded bars under the trade name as Dywidag® 15/17 was used to attach the confining stress-inducing system as captured in Figure 4(b). Two displacement transducers were placed on both sides of the specimens as shown in Figure 4(c) to measure an average vertical displacement due to applied force. An applied load was monotonically increased up to the failure of the tested specimens.

Experimental Results

Load and displacement levels of all specimens are presented in Table 3. It is noted that three replicated specimens were tested in cases of NC-0.5SF and NC-1SF. The considered load levels include the cracking load (V_{cr}), maximum shear force ($V_{\max}$), and residual strength (V_r). The cracking load was identified by the presence of the first crack observed in tested specimens. The residual strength refers to shear force at 20% load decrease after reaching the maximum load. The cracking load ratio is defined as the ratio between V_{cr} and $V_{\max}$. The residual strength ratio is V_r divided by $V_{\max}$. The cracking load ratio of the specimen NC was 0.71.

Table 3. Experimental Results of Tested Specimens

Specimen	V_{cr} (kN)	$V_{\max}$ (kN)	V_r (kN)	u_{cr} (mm)	$u_{\max}$ (mm)	u_r (mm)
NC	268.2	378.7	310.5	0.51	0.96	1.26
NC-0.5SF-1	231.1	338.7	277.7	1.05	1.49	2.22
NC-0.5SF-2	243.4	353.6	287.3	0.68	1.32	2.12
NC-0.5SF-3	260.6	368.8	315.9	0.43	0.99	1.21
NC-1SF-1	320.4	445.6	356.3	0.55	1.31	2.58
NC-1SF-2	342.2	483.2	392.6	0.87	1.60	2.49
NC-1SF-3	380.2	593.1	545.1	1.17	2.02	2.59
HC	165.7	326.4	265.3	0.84	1.48	1.62

The displacement levels are presented in the same manner with the considered load levels. The displacement at cracking load (u_{cr}), displacement at maximum load ($u_{\max}$), and displacement at residual strength (u_r) are determined. The ductility index at maximum load is defined as the ratio between $u_{\max}$ and u_{cr}. The ductility index at residual strength is calculated by dividing u_r by u_{cr}. The specimen NC has a ductility index at maximum load and residual strength of 1.88 and 2.47, respectively.

Shear Force - Vertical Displacement Relationship

Figure 5 compares the shear force-displacement curves of the specimens with different compressive strength classes. The cracking load ratio of the specimen HC is 0.51. Despite the increase in concrete compressive strength, the cracking load ratio of the specimen HC decrease by 28%, compared to those of the specimen NC. The results indicate that maximum load of the tested specimen did not significantly change with the increase in concrete compressive strength. This may be due to minimum number of specimen HC. In order to clarify the behavior of high-strength special dry joint, it is recommended that forthcoming experiments shall focus on special dry joint with a concrete compressive strength higher than 50 MPa.

The ductility index at maximum load and residual strength of the specimen HC are 1.76 and 1.93, respectively. The enhancement in concrete compressive strength by 55% shows a lower ductility index at maximum load by 6%. Also, the ductility index at residual strength of the specimen HC is lower than that of the specimen NC by 28%.

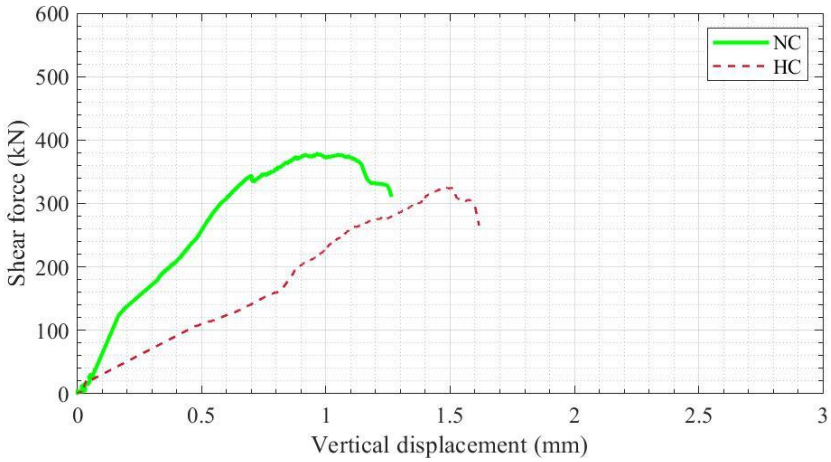

Figure 5. Effect of concrete compressive strength on shear force-displacement curve

The effect of steel fiber volume on shear force-displacement curve of the tested specimens is shown in Figure 6. Cracking load ratio and ductility index of three identical specimens are averaged then compared. The specimen NC-0.5SF and NC-1SF provided the same cracking load ratio at 0.69. These results indicate that the cracking load ratio is not affected by the addition of steel fibers between 0.5% and 1%. However, as presented in Figure 6, the maximum load is found to increase approximately 34% compared with the specimen NC when 1% of steel fiber is used.

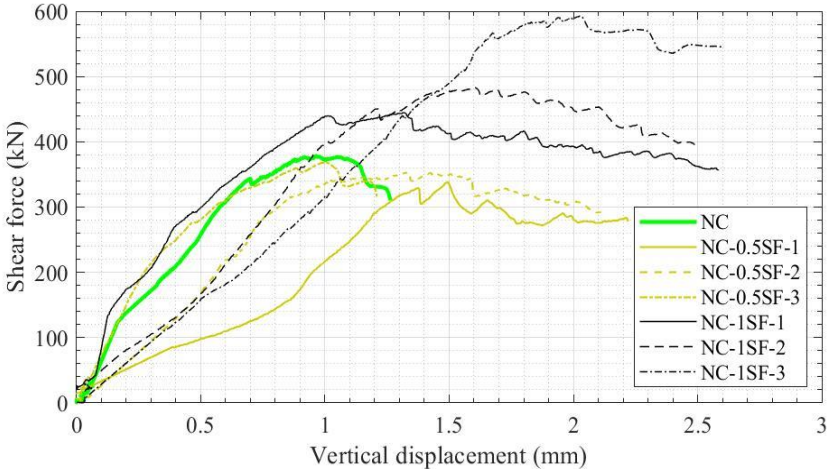

Figure 6. Effect of steel fiber volume on shear force-displacement curve

The ductility index at maximum load and residual strength of specimen NC-0.5SF are 1.90 and 2.68, respectively. The specimen NC-1SF has a ductility index at maximum load and residual strength of 1.98 and 3.26, respectively. The results show that the ductility index at maximum load and residual strength significantly increase with the increase in steel fiber volume.

Damage Pattern

The crack-initiation patterns of the specimens are illustrated in Figure 7. An initial crack was usually observed in male part. The shear stress may be mainly concentrated at the male part rather than the female part of the special dry joints. In addition, it was observed that, in most specimens, crack initiated at approximately 70% of the maximum applied load. However, crack of the specimen HC formed after an applied load reached 50% of the maximum applied load. The inclusion of steel fibers and the increase of concrete compressive strength could not delay cracking load.

An experimental result showed that the initial cracks propagated along the plane at around 45 degrees to the applied load, as shown in Figure 7. Cracks widened as applied load increased. The crack patterns at maximum load were illustrated in Figure 8. Many crack paths were intimately connected to produce shearing off failure. According to the experiment, the specimens with steel fibers exhibited a slower crack propagation compared to the specimen NC and HC. This crack bridging action due to the use of fiber in concrete is consistent with earlier evidence reported by the literatures [18, 30-32]. A widespread cracking was observed over the shear key region only in case of the specimens with steel fibers.

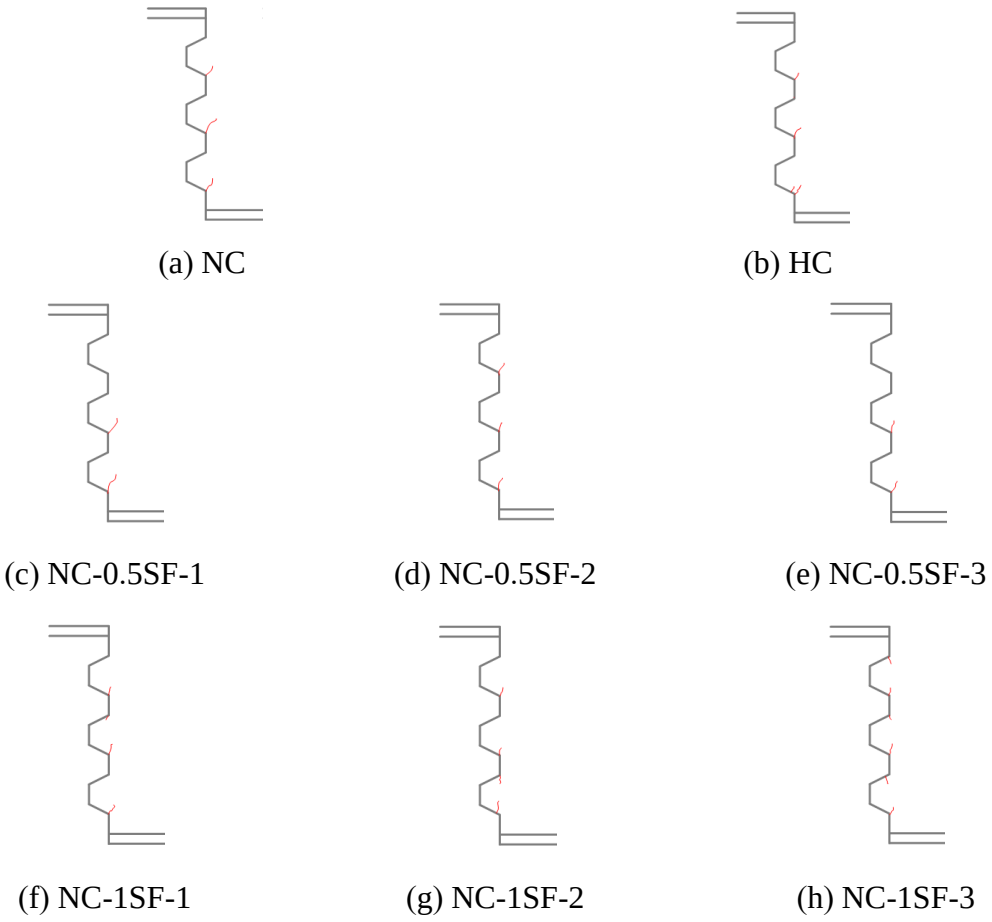

Figure 7. Crack initiation of the specimens (not to scale)

The failure patterns for all specimens are depicted in Figure 9. The failure mode of the specimen NC and HC are a typical pattern which is the shearing-off of a male part of the dry joint.

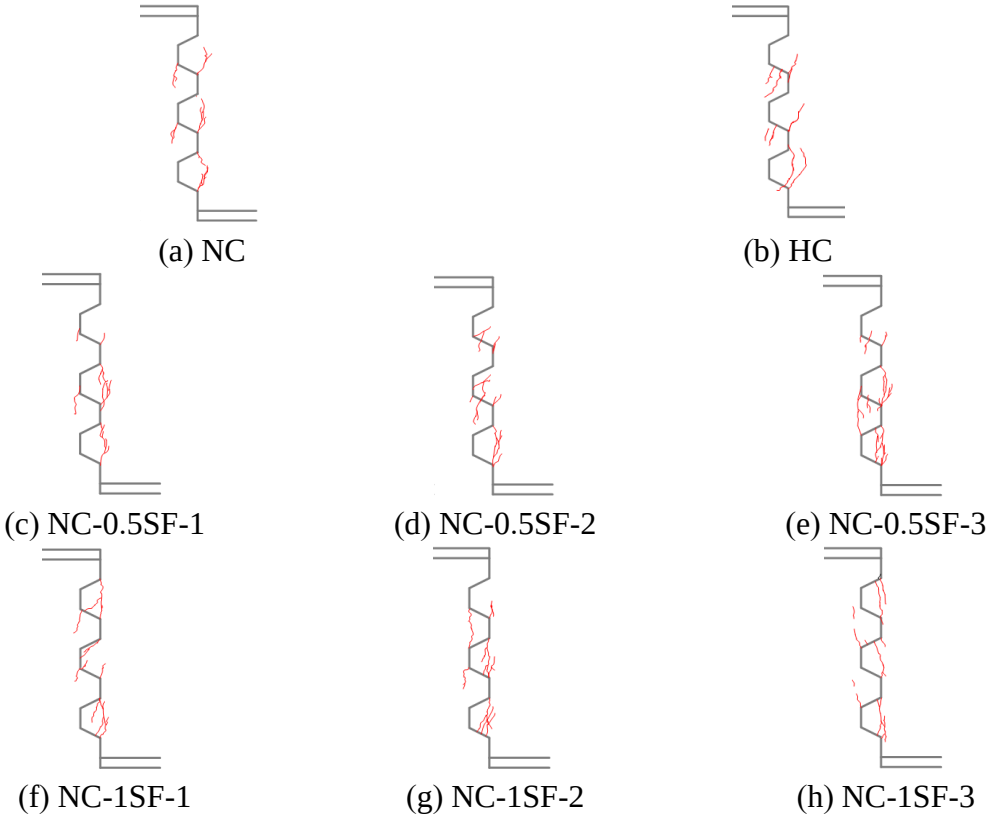

(a) NC (b) HC

(c) NC-0.5SF-1 (d) NC-0.5SF-2 (e) NC-0.5SF-3

(f) NC-1SF-1 (g) NC-1SF-2 (h) NC-1SF-3

Figure 8. Crack formation at maximum load (not to scale)

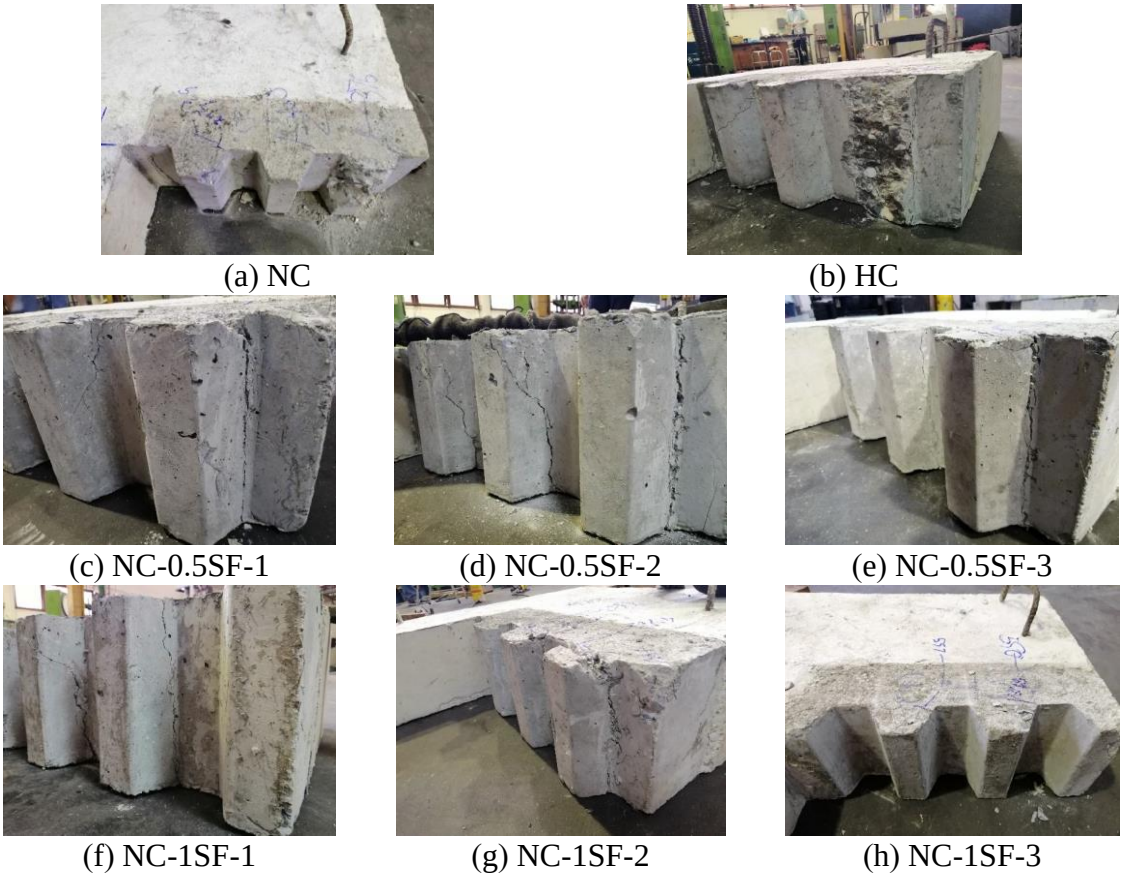

(a) NC (b) HC

(c) NC-0.5SF-1 (d) NC-0.5SF-2 (e) NC-0.5SF-3

(f) NC-1SF-1 (g) NC-1SF-2 (h) NC-1SF-3

Figure 9. Failure of tested specimens

This suggested that the concrete compressive strength has insignificant effect on failure mode of specimen. On the other hand, the ductile shearing-off failure was found in the specimens with steel fibers. The specimens with steel fibers showed sign of concrete cracking around shear key corners. This indicates that adding steel fibers changed the failure mode of the specimens from shearing-off to ductile shearing-off.

Evaluation of Shear Capacity

The existing equations for shear capacity of keyed joints (V_j) from literatures are summarized in Table 4. The SI unit system is used in all equations. Each equation consists of three different input geometric parameters (A_j, A_k, and A_{sm}). A_j denotes the total area of joint surface. A_k and A_{sm} are the base areas of all keys in the failure plane and contact area between smooth surfaces on failure plane, respectively. As seen from Table 4, most of the equations for shear capacity depend on concrete compressive strength (f_c') and confining stress (σ_n) except for the equation proposed by Alcalde et al. [26]. The equation suggests that the shear capacity is influenced by the number of keys in a male part of joint (n_k). It is noted that the equation developed by Alcalde et al. [26] is valid only for f_c' of 50 MPa and σ_n presenting less than 3 MPa. Moreover, the equation proposed by Turmo et al. [19] is valid only for the concrete compressive strength up to 50 MPa.

Table 4. Equations of Shear Capacities of Keyed Joints Proposed in Literatures

Reference	Equations for Shear Capacity of Keyed Joints	Eq.
Buyukozturk et al., 1990 [13]	$V_j = A_j(0.65\sqrt{f_c'} + 1.36\sigma_n)$	(1)
AASHTO, 1998 [33]	$V_j = A_k\sqrt{f_c'}(1 + 0.205\sigma_n) + (0.6A_{sm}\sigma_n)$	(2)
Rombach and Specker, 2004 [34]	$V_j = 0.14 f_c' A_k + 0.65\sigma_n A_j$	(3)
Turmo et al., 2006 [19]	$V_j = A_k \frac{\sqrt[3]{(f_c')^2}}{100}(33 + 7\sigma_n) + (0.6A_{sm}\sigma_n)$	(4)
Alcalde et al., 2013 [26]	$V_j = 7.118A_k(1 - 0.064n_k) + 2.436A_{sm}\sigma_n(1 + 0.127n_k)$	(5)

Note: A_j is the total area of joint surface, A_k is the base areas of all keys in the failure plane, A_{sm} is the area of contact between smooth surfaces on the failure plane, f_c' is concrete compressive strength, σ_n is confining stress, and n_k is number of keys in a male part of joint.

Shear capacities calculated from aforementioned equations are compared with the experimental results, as shown in Figure 10 and Table 5. It is noted that, in case of specimen HC, the shear capacities are estimated by Eqs. (1)-(3) only because the concrete compressive strength of specimen HC exceeds the applicable range of Eqs. (4) and (5). It is found that Eqs. (1)-(3) overestimate the shear capacity of the specimen HC by 99-114% compared with the experimental result as seen from the outermost left data in Figure 10. This means that Eqs. (1)-(3) are not applicable to predict shear capacity in the case of the specimen HC. As a result, the ratios between estimated shear capacity and experimental shear capacity of the specimen HC are excluded from Table 5. This would prevent bias arising from limitation of equations developed by Turmo et al. [19] and Alcalde et al. [26].

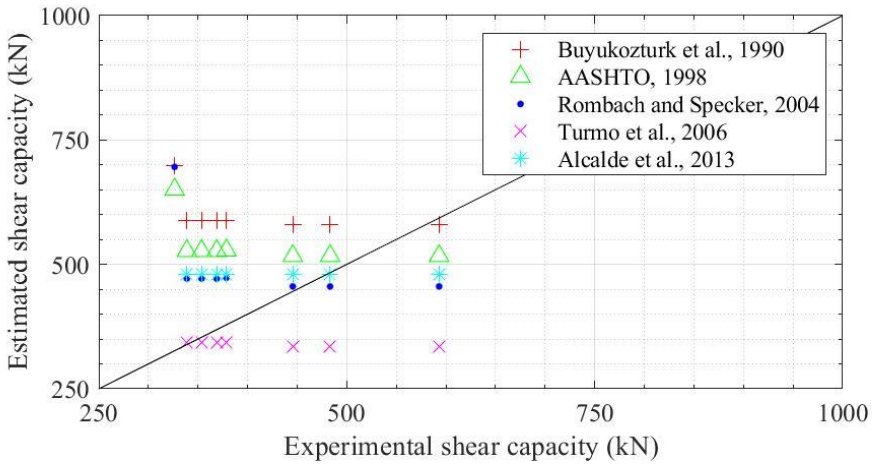

Figure 10. Comparison of estimated shear capacities with experimental results

Table 5. Estimated Result to Experimental Result Ratios of Normal Strength Specimens

Specimen	Buyukozturk et al. [13]	AASHTO [33]	Rombach and Specker [34]	Turmo et al. [19]	Alcalde et al. [26]
NC	1.56	1.39	1.25	0.91	1.27
NC-0.5SF-1	1.74	1.56	1.39	1.01	1.42
NC-0.5SF-2	1.66	1.49	1.33	0.97	1.36
NC-0.5SF-3	1.59	1.43	1.28	0.93	1.30
NC-1SF-1	1.30	1.16	1.02	0.75	1.08
NC-1SF-2	1.20	1.07	0.94	0.69	0.99
NC-1SF-3	0.98	0.87	0.77	0.56	0.81
Average	1.43	1.28	1.14	0.83	1.17
S.D.	0.28	0.25	0.23	0.17	0.22

Based on the data Table 5, Turmo's equation (Eq.(4)) provides the best prediction of shear capacity for the specimen NC. Equations (1)–(3) and (5) which were developed by the literatures [13, 26, 33, 34] overestimate the shear capacity of the specimen NC by 25-56% compared with the experimental results. This reveals that these equations (Eqs. (1)–(3) and (5)) are not appropriate to predict shear capacity of the special dry joints.

Regarding to the special dry joint with steel fibers, the predicted shear capacities of the specimens with 0.5% steel fiber volume using Turmo's equation are still closed to the experimental results. However, for the specimens with 1% steel fiber volume, the predicted shear capacities using Turmo's equation are underestimated by 25-44% compared with the experimental results. Based on the results of seven specimens, the Turmo's equation yields the lowest deviation compared to other equations. Nevertheless, the equations proposed in the literatures do not account for the effect of steel fiber volume on shear capacity of the special dry joints. A development of shear capacity equation for the special dry joints using steel fiber reinforced concrete with compressive strength of more than 50 MPa requires future investigation.

Conclusions

This study investigated the effect of concrete compressive strength and steel fiber volume on shear behavior of the proposed special dry joint for precast segmental concrete members. Shear capacity equations in literatures were validated against the experimental results. Based on the study, the conclusions can be drawn as follows:

1. The special dry joints without steel fiber were failed by shearing off of the shear keys.
2. The maximum load of the specimens and ductility index were improved more prominently when the 1% of steel fibers was added in the special dry joints. Moreover, the addition of steel fibers changed the failure mode of the specimens from shearing off to ductile shearing-off failure.
3. Among the existing shear capacity equations, the equation proposed by Turmo et al. [19] provides reasonable prediction of shear capacity of the normal strength-special dry joint without steel fibers. The equation, however, underestimates the shear capacity of specimens with 1% steel fibers. This is because the effect of steel fibers is not considered in the equation.

References

[1] H. Jang, H. S. Lee, K. Cho, and J. Kim, "Experimental study on shear performance of plain construction joints integrated with ultra-high performance concrete (UHPC)," *Construction and Building Materials,* Vol. 152, pp. 16-23, 2017. doi: http://dx.doi.org/10.1016/j.conbuildmat.2017.06.156

[2] C. Li, Z. Feng, L. Ke, R. Pan, and J. Nie, "Experimental study on shear performance of cast-in-place ultra-high performance concrete structures," *Materials,* Vol. 12, pp. 1-16, 2019. doi: http://doi:10.3390/ma12193254

[3] H. Jang, H. S. Lee, K. Cho, and J. Kim, "Numerical and experimental analysis of the shear behavior of ultrahigh-performance concrete construction joints," *Advances in Materials Science and Engineering,* Vol. 2018, No. 6429767, 2018. doi: https://doi.org/10.1155/2018/6429767

[4] B.A. Gopal, F. Hejazi, M. Hafezolghorani, and V.Y. Lei, "Numerical analysis and experimental testing of ultra-high performance fibre reinforced concrete keyed dry and epoxy joints in precast segmental bridge girders," *International Journal of Advanced Structural Engineering,* 2019. doi: http://doi.org/10.1007/s40091-019-00246-6

[5] M.A. Issa, and H.A. Abdalla, "Structural behavior of single key joints in precast concrete segmental bridges," *Journal of Bridge Engineering,* Vol. 12, No. 3, pp. 315-324, 2007. doi: http://10.1061/(ASCE)1084-0702(2007)12:3(315)

[6] H.S. Kim, W.J. Chin, J.R. Cho, Y.J. Kim, and H. Yoon, "An experimental study on the behavior of shear keys according to the curing time of UHPC," *Engineering,* Vol. 7, pp. 212-218, 2015. doi: http://dx.doi.org/10.4236/eng.2015.74017

[7] X. Zhou, N. Mickleborough, and Z. Li, "Shear strength of joints in precast concrete segmental bridges," *ACI Structural Journal,* Vol. 102, No. 1, pp. 3-11, 2005.

[8] A.A. Semendary, W.K. Hamid, E.P. Steinberg, and I. Khoury, "Shear friction performance between high strength concrete (HSC) and ultra high performance concrete (UHPC) for bridge connection applications," *Engineering Structures,* Vol. 205, p. 110122, 2020. doi: http://doi.org/10.1016/j.engstruct.2019.110122

[9] Z.Y. Bu, and W.Y. Wu, "Inter shear transfer of unbonded prestressing precast segmental bridge column dry joints," *Engineering Structures,* Vol. 154, pp. 52-65, 2018. doi: http://dx.doi.org/10.1016/j.engstruct.2017.10.048

[10] H. Jiang, J. Feng, A. Liu, W. Liang, Y. Tan, and H. Liang, "Effect of specimen thickness and coarse aggregate size on shear strength of single-keyed dry joints in precast concrete segmental bridges," *Structural Concrete,* Vol. 20, pp. 955-970, 2019. doi: http://doi.org/10.1002/suco.201800054

[11] T. Liu, Z. Wang, J. Guo, and J. Wang, "Shear strength of dry joints in precast UHPC segmental bridges: experimental and theoretical research," *Journal of Bridge Engineering,* Vol. 24, No. 1, p. 04018100, 2019. doi: http://doi.org/10.1061/(ASCE)BE.1943-5592.0001323

[12] I.S. Ibrahim, K.H. Padil, H.M. A. Bady, A.A. Saim, and N.N. Sarbini, "Ultimate shear capacity and failure of shear key connection in precast concrete construction," *Malaysian Journal of Civil Engineering*, Vol. 26, No. 3, pp. 414-430, 2014.
[13] O. Buyukozturk, M.M. Bakhoum, and S.M. Beattie, "Shear behavior of joints in precast concrete segmental bridges," *Journal of Structural Engineering*, Vol. 116, pp. 3380-401, 1990. doi: http://doi.org/10.1061/(ASCE)0733-9445(1990)116:12(3380)
[14] H.H. Hung, Y.C. Sung, K.C. Lin, C.R. Jiang, and K.C. Chang, "Experimental study and numerical simulation of precast segmental bridge columns with semi-rigid connections," *Engineering Structures*, Vol. 136, pp. 12-25, 2017. doi: https://dx.doi.org/10.1016/j.engstruct.2017.01.012
[15] M.R. LeBorgne and R.M. Gutkowski, "Effects of various admixtures and shear keys in wood-concrete composite beams," *Construction and Building Materials*, Vol. 24, pp. 1730-1738, 2010. doi: https://10.1016/j.conbuildmat.2010.02.016
[16] A. Vasseghi, "Energy dissipating shear key for precast concrete girder bridges," *Scientia Iranica Transactions A: Civil Engineering*, Vol. 18, No. 3, pp. 296-303, 2018. doi: https://10.1016/j.scient.2011.05.036
[17] W. Pattharakorn, *A Study for Shear Resisting Behavior of Special Dry Joints for Precast Prestressed Concrete Reinforced with Steel Fiber*, Thesis (Master's), Chulalongkorn University, 2018.
[18] H. Jiang, R. Wei, Z.J. Ma, and Y. Li, "Shear strength of steel fiber-reinforced concrete dry joints in precast segmental bridges," *Journal of Bridge Engineering*, Vol. 21, No. 11, p. 04016085, 2016. doi: http://10.1061/(ASCE)BE.1943-5592.0000968
[19] J. Turmo, G. Ramos, and A.C. Aparicio, "Shear strength of dry joints of concrete panels with and without steel fibres: application to precast segmental bridges," *Engineering Structures*, Vol. 28, pp. 23-33, 2006.
doi: http://doi:10.1016/j.engstruct.2005.07.001
[20] F. Hanif, and T. Kanakubo, "Shear performance of fiber-reinforced cementitious composites beam-column joint using various fibers," *Journal of the Civil Engineering Forum*, Vol. 3, No. 2, 2017. doi: https://doi.org/10.22146/jcef.26571
[21] X. Yan, S. Wang, C. Huang, A. Qi, and C. Hong, "Experimental study of a new precast prestressed concrete joint," *Applied Sciences*, Vol. 8, No. 1871, 2018. doi: https://10.3390/app8101871
[22] S.A. Wulan, I. Satyarno, and A. Saputra, "Mix design of self compacting concrete based on ultra high compressive strength flow mortar mix," *Journal of the Civil Engineering Forum*, Vol. 4, No. 1, 2018. doi: https://doi.org/10.22146/jcef.29797
[23] J. Turmo, G. Ramos, and Á.C. Aparicio, "Shear behavior of unbonded post-tensioned segmental beams with dry joints," *ACI Structural Journal*, Vol. 103, No. 3, pp. 409-417, 2006.
[24] S. Singhal and A. Chourasia, "Joint connections for precast structural concrete components," In: *16th Symposium on Earthquake Engineering*, Indian Institute of Technology, Roorkee, India, 2018.
[25] American Society for Testing and Materials (ASTM), *Standard Specification for Deformed and Plain Carbon-Steel Bars for Concrete Reinforcement (ASTM A615 / A615M-18e1)*, West Conshohocken, Pennsylvania, United States, 2018.
[26] M. Alcalde, H. Cifuentes, and F. Medina, "Influence of the number of keys on the shear strength of post-tensioned dry joints," *Materiales de Construcción*, Vol. 63, No. 310, pp. 297-307, 2013. doi: http://doi.org/10.3989/mc.2013.07611
[27] W. Smittakorn, P. Manavithayarak, and P. Sukmoung, "Improvement of shear capacity for precast segmental box girder dry joints by steel fiber and glass fiber," *MATEC Web of Conferences*, Vol. 258, No. 04006, 2018.

doi: https://doi.org/10.1051/matecconf/201925804006
[28] H.H. Hussein, S.M. Sargand, F. T. Al Rikabi, and E. P. Steinberg, "Laboratory evaluation of ultrahigh-performance concrete shear key for prestressed adjacent precast concrete box girder bridges," *Journal of Bridge Engineering*, Vol. 22, p. 04016113, 2017. doi: https://doi:10.1061/(ASCE)BE.1943-5592.0000987
[29] Transportation Research Board, *Adjacent Precast Concrete Box Beam Bridges: Connection Details*, Washington, 2009.
[30] Z. Xu, Wenyin, and Y. Liang, "Experimental study of steel fibre bridging action on crack propagation in fibre reinforced concrete," *Key Engineering Materials*, Vol. 324-325, pp. 1067-1070, 2006. doi: https://10.4028/www.scientific.net/KEM.324-325.1067
[31] R.S. Olivito, and F.A. Zuccarello, "An experimental study on the tensile strength of steel fiber reinforced concrete," *Composites: Part B*, Vol. 41, pp. 246-255, 2010. doi: https://10.1016/j.compositesb.2009.12.003
[32] Z.X. Li, C.H. Li, and J.B. Yan, "Seismic behaviour of hybrid-fibre reinforced concrete shear keys in immersed tunnels," *Tunnelling and Underground Space Technology*, Vol. 88, pp. 16-28, 2019. doi: https://doi.org/10.1016/j.tust.2019.02.022
[33] American Association of State Highway and Transportation Officials (AASHTO), *Guide Specifications for Design and Construction of Segmental Concrete Bridges*, Washington, United States, 1998.
[34] G. Rombach, and A. Specker, "Segmentbrücken," In *Beton-Kalender Teil 1*, K. Bergmeister and J.D. Wörner, eds.: Berlin, Germany, pp. 177-211, 2004.